Adele Cutignano–Conceptualization, Data Curation, Formal analysis; Investigation; Methodology; Resources, Supervision, Writing - original draft, review & editing.

Gianluca Picariello – Conceptualization, Data Curation, Formal analysis; Investigation; Methodology; Resources, Supervision, Writing - original draft, review & editing.

Floriana Boscaino, -Investigation and Methodology

Marco Maccaferri -Investigation and Methodology

Gianfranco Mamone - Funding acquisition

Aldo Ceriotti- Funding acquisition

1. UHPLC-HRESI-MS/MS
2. LipidSearch identification

Q-Exactive platform

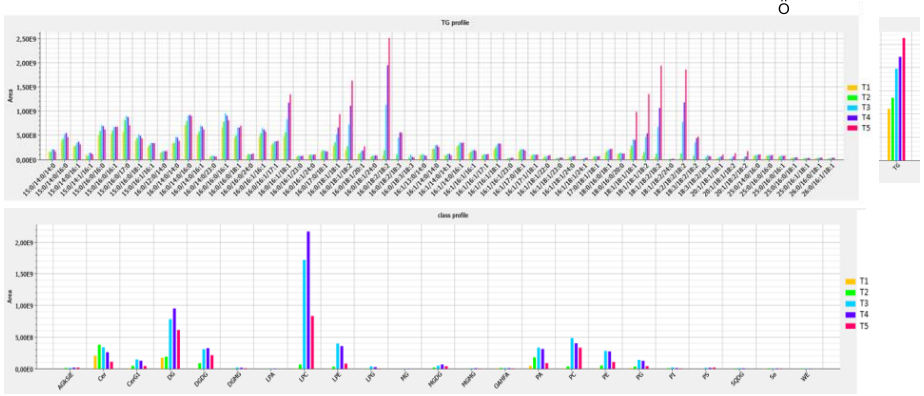

TG

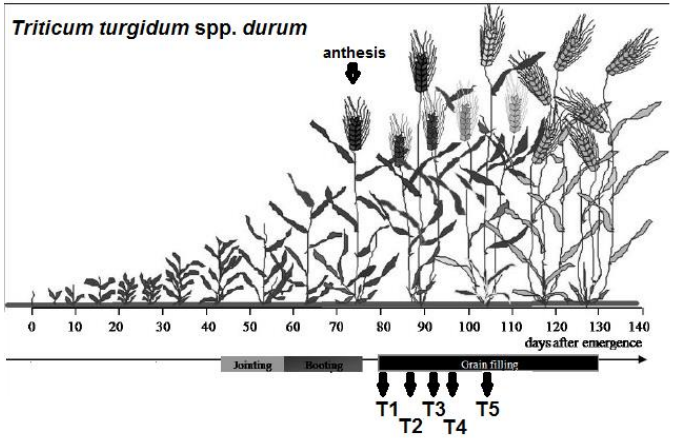

PL

LysoPL

GL

AGlcSiE

SP

Monitoring changes of lipid composition in durum wheat during grain development

Adele Cutignano[a,*] Gianfranco Mamone[b], Floriana Boscaino[b], Aldo Ceriotti[c], Marco Maccaferri[d], Gianluca Picariello[b,*]

[a]*Istituto di Chimica Biomolecolare (ICB), Consiglio Nazionale delle Ricerche (CNR), via Campi Flegrei, 34 - 80078 Pozzuoli (Napoli), Italy*

[b]*Istituto di Scienze dell'Alimentazione (ISA), Consiglio Nazionale delle Ricerche (CNR), via Roma, 64 - 83100 Avellino, Italy*

[c]*Istituto di Biologia e Biotecnologia Agraria (IBBA), Consiglio Nazionale delle Ricerche (CNR), via Edoardo Bassini, 15 - 20133 Milano, Italy*

[d]*Dipartimento di Scienze e Tecnologie Agroalimentari (DISTAL), Università di Bologna, viale Giuseppe Fanin, 44 - 40127 Bologna, Italy*

*Corresponding authors.

Adele Cutignano. Email: acutignano@icb.cnr.it

Tel +39 081 8675313; Fax +39 081 8041770

Gianluca Picariello. Email: picariello@isa.cnr.it

Tel +39 0825 299521; Fax +39 0825 781585

Abstract

The lipid fraction of durum wheat (*Triticum turgidum* ssp. *durum* (Desf.) Husn.), cultivar Svevo, was characterized during grain maturation. Growing grain kernels were harvested at five key stages of development

between 5 and 30 days post anthesis (dpa). Lipid evolution was assessed during kernel filling by gas chromatography-mass spectrometry (GC-MS) analysis of triacylglycerols and methylated free fatty acids (FFA) as well as by ultra-high performance liquid chromatography coupled to high resolution electrospray ionization tandem mass spectrometry (UHPLC-HRESI-MS/MS) lipid analysis. Major triacylglycerols (TAG) were detected already at early developmental stages, albeit at low abundance. The decrease of FFA during kernel filling corresponded to accumulation of predominantly linoleate (C18:2n6)-containing C52 and C54 TAG. Fatty acid composition of polar lipids including phospholipids and galactolipids also showed the progressive dominance of linoleate, typically since two weeks after anthesis. Conversely, minor sphingolipids (ceramides and glycosylceramides) were constituted mainly by saturated long chain FA, also oxygenated, combined with a restricted set of sphingoid bases, and might play a signaling role during grain development.

Keywords: *Triticum turgidum* ssp. *durum* (Desf.) Husn., durum wheat, grain maturation, lipidomics, mass spectrometry, Q Exactive

1. Introduction

Cereals represent staple crops worldwide and the main source of food for humankind. Among them, wheat (*Triticum* spp.) plays a central role as it is transformed in flour that is used to prepare bread, pasta, pizza and a huge variety of baked foods. Based on the genetic asset, wheat is commonly classified as soft (*Triticum aestivum* L.) or durum (*Triticum turgidum* ssp. *durum* (Desf.) Husn.). Genomic differences determine distinct biochemical composition in terms of starch, proteins and lipids, rendering soft wheat flour mainly suited for the preparation of bread and baked products and durum wheat for making semolina and pasta.

Durum wheat has a tetraploid AABB genome (4 x 7, 4*n*). The ancient domestication and the subsequent breeding practices have selected the modern durum wheat, under the pressure of agronomical behavior and, more recently, pasta quality features. The main technological properties of durum wheat affecting pasta

48 quality are undoubtedly related to the starch and protein content. However, minor components of the wheat
49 caryopsis, such as lipids and xanthophylls, significantly affect nutritional and technological traits: for instance,
50 nonpolar lipids influence the rate of starch gelatinization in pasta, glycolipids act as endogenous surfactants in
51 dough, while carotenoids determine the “yellow index” of durum wheat.
52 On average, the lipid content of wheat kernels varies within the 2.4-3.8 % range (as dry weight), depending on
53 the cultivar and abiotic factors (Lafiandra et al., 2012). Durum wheat contains slightly higher levels of lipids
54 than the soft counterpart. Lipids are unevenly distributed in the caryopsis, as they are particularly concentrated
55 in the embryo (germ) and in the outer teguments. However, outer layers and embryo of the mature wheat
56 caryopsis account for only 7–8% and nearly 6.0 % of the dry weight, respectively. Nevertheless, the nutritional
57 value as well as the cancer chemopreventing and antioxidant properties of lipids they contain have attracted
58 increasing interest (González-Thuillier et al., 2015; Mahmoud et al., 2015). The greatest kernel compartment is
59 represented by the starchy endosperm (80-83%) which is low in lipids, while the protein-rich aleurone layer
60 constitutes about 6.5% of the caryopsis (Barron et al., 2007). Within the endosperm, lipid concentration
61 progressively decreases from the outer to the inner layers (Liu, 2011).
62 Generally, when the grain is milled and sieved, outer layers, germ and aleurone are removed and recovered
63 together as the bran, thereby lowering the lipid content of refined flour or semolina up to 1.0-1.5 % dry weight.
64 During milling, lipids partly migrate from the germ and aleurone to the endosperm particles and they
65 redistribute with a fairly constant ratio of neutral, phospho- and glyco-lipids (Morrison, 1994). Despite their low
66 content, lipids significantly impact functionality of flour and dough by interacting with gluten proteins and
67 starch. In particular, polar lipids (i.e. glycolipids and phospholipids) seem to be favorable to baking
68 performance while nonpolar lipids (i.e., triacylglycerols, TAG) and free fatty acids (FFA) appear to be
69 detrimental (MacRitchie, 1977). Furthermore, lipids influence processing and storage properties of cereal-
70 based products. Pioneering works carried out in 60’s by thin layer chromatography (TLC) and chemical analysis
71 highlighted the gross changes in lipid composition during wheat maturation (Daftary and Pomeranz, 1965;
72 Klopfenstein and Pomeranz, 1968). Afterwards, wheat lipids were characterized by combining chromatographic

fractionation and GC analysis (Stokes et al., 1986). The assessment of the galactolipid content enabled discrimination between T*. durum* and *T. aestivum* (Qin et al., 2019). Recent mass spectrometry (MS)-based lipidomic investigations addressed the qualitative and quantitative determination of lipid classes and FFA content (Geng et al., 2015; González-Thuillier et al., 2015; Narducci et al., 2019; Wetzel et al., 2014), providing more detailed information about lipid distribution in wheat grain compartments. However, most of MS-based studies have explored only the lipid composition of mature wheat kernels, while the evolution of class-specific FA-composition during grain filling has not been investigated in detail, so far.

The complete genome of durum wheat has been recently sequenced and released, utilizing the Svevo accession, chosen as a reference cultivar (Maccaferri et al., 2019). Metabolic and storage proteins of the same accession have been recently characterized by proteomic approaches (Arena et al., 2017; Mazzeo et al., 2017). As a part of a large research project aimed at defining the global biomolecular asset by state-of-the-art integrated omic technologies, herein the lipid fraction of Svevo durum wheat was characterized during grain maturation. Plants were grown under controlled conditions and filling grains were collected at various stages of development between 5 and 30 days post anthesis (dpa) to assess lipid evolution by ultra-high performance liquid chromatography coupled to high resolution tandem mass spectrometry (UHPLC-HRESI-MS/MS), with special focus on acylglycerides, glycolipids, phospholipids and FFA.

2. Material and methods

2.1 Plant material

Durum wheat cultivar Svevo was experimentally grown in early spring 2015 in a growth chamber under completely controlled conditions of photoperiod, air, temperature and humidity, as well as horizontal laminar air flux, as previously detailed (Mazzeo et al., 2017). The growing cycle lasted for three months. Developing kernels were harvested at specific developmental stages, namely at 5 (embryo increase and kernel development at 1/3 of full developmental size, water-ripening stage), 11 (half-full size, water-ripening stage),

16 (kernel full development, water-ripening stage), 21 (milk-ripening stage) and 30 (dough stage) dpa, according to typical reference stages (CerealDB, http://bio-gromit.bio.bris.ac.uk/cerealgenomics/cgi-bin/grain3.pl). Samples were harvested in triplicate and are named as follows: 5 dpa (T1), 11 dpa (T2), 16 dpa (T3), 21 dpa (T4) and 30 dpa (T5). Immediately after harvesting, developing kernels were stored at -80 °C.

2.2 Sample preparation

Whole kernels were lyophilized, ground to a powder using a mortar and the obtained lyophilized powder kept frozen at -26°C until analyses. Lipids were extracted adapting the Bligh and Dyer method of total lipid extraction. Briefly, 100 mg aliquots of kernel powder were extracted in glass vials, according to the following steps: addition of 0.2 mL water and vortexing 10 min to form a wet slurry; addition of 0.75 mL chloroform–methanol (1/2, v/v) and 10–15 min vortexing; addition of 0.25 mL chloroform and vortexing for 5 min; addition of 0.25 mL water and vortexing for 5 min; centrifugation for 10 min (3000×g, 4 °C, 15 min). The lower organic layer was collected by aspiration. The aqueous phase was discarded as no lipids were detected by TLC, while the pellet and interfacial layer were re-extracted twice with the same procedure described above. The organic extracts were combined, dried under N_2 stream and stored at -80 °C until use. The yields of lipidic extracts from 100 mg of lyophilized kernels from each sampling period were: 1.0 mg (T1), 2.3 mg (T2), 3.6 mg (T3), 3.8 mg (T4) and 1.7 mg (T5).

2.3 High performance thin layer chromatography (HPTLC)

Before analysis lipids were re-dissolved in 1 mL of chloroform–methanol (2:1, v/v) and aliquoted. Lipid extracts were separated by HPTLC using silica gel 60 plates (Merck, Darmstadt, Germany), placing 2 µL of solution for each T1-T5 sample. TAG-rich wheat germ oil, purchased at a local herbalist's shop, was run by comparison. The developing eluent was petroleum ether/diethyl ether (80:20, v/v). Lipids were visualized by exposure to iodine vapors or by charring the plates previously sprayed with 10% (w/v) phosphomolybdic acid in ethanol.

2.4 TAG analysis by GC-MS

Raw extracts from each sampling were dried and resuspended in 2 mL of *n*-heptane. Each sample was analyzed using a gas chromatograph (model 7890 A; Agilent Technologies, Santa Clara, CA) coupled with a quadrupole mass spectrometer 5975 C (Agilent). Separation was carried out with a Rtx-65TG (mod. 17008) capillary column (30 m x 0.25 mm i.d.; 0.10 mm film thickness) from Restek (Bellefonte, PA, USA). High-purity helium was used as the gas carrier at 0.80 mL/min. Samples (1 µL) were injected through an MPS2 autosampler (Gerstel, Mülheim an der Ruhr, Germania) at 370 °C in splitless mode. Experimental chromatographic conditions were as follows: the initial temperature (220°C) was raised to 320 °C at a rate of 15°C /min and then to 355°C at a rate of 7°C /min, holding at 355°C for 20 min. Spectra were recorded in full scan mode from 29 *m/z* to 1050 *m/z* with 0.2 s/scan. TAG were identified through the mass spectra, by matching with previous data reporting the expected species and comparing the retention times with an in-house developed retention time library based on commercial standards. The results are the average of three replicates, expressed as area percentage.

2.5 Free fatty acid methyl ester (FAME) analysis by GC-MS

A small aliquot corresponding to 1/10 of lipid extract from each harvested sample was methylated with ethereal diazomethane (CH_2N_2) freshly prepared from DIAZALD® (*N*-methyl-*N*-nitroso-*p*-toluenesulfonamide) by using a glassware apparatus obtained from Aldrich (Merck Life Science, Milano, Italy; Macro Diazald® Kit, Cat. No. Z100250). Each T1-T5 aliquot was dissolved in methanol (MeOH, 200µL) in a glass vial and 1mL of a cold ethereal solution of CH_2N_2 was added. The reaction mixture were left at r.t. for 3 hrs. Samples were successively dried under N_2 stream and redissolved in MeOH (200 µL) before GC-MS analysis (2 µL sample injection volume) with an ion-trap MS instrument in EI mode (70 eV) (Thermo, Polaris Q) connected with a GC system (Thermo, GCQ) by a 5% phenyl/methyl polysiloxane column (30 m × 0.25 mm × 0.25 µm, Agilent, VF-5ms) using high-purity helium as the gas carrier. The following temperature gradient was applied: Initial 160 °C holding for 3 min; then 5°C/min up to 260 °C followed by 30 °C/min up to 310°C, holding for 3 min at 310 °C; split flow 10 mL/min; full scan m/z 50–450. FAME were identified by comparison with authentic standards.

147

148 *2.6 Lipid analysis by UHPLC-Q Exactive-ESI-MS/MS*

149 Crude lipid extracts obtained by equal amount of cereal grains for each sampling time as described above were
150 dissolved in 1 mL MeOH/Isopropanol 50:50 (v/v) and diluted 1:20 in the LC-MS initial elution solvent.
151 Chromatographic separation was performed on an Infinity 1290 UHPLC System (Agilent Technologies, Santa
152 Clara, CA, USA), equipped with a Kinetex Biphenyl column (2.6 µm, 150 × 2.1 mm) (Phenomenex, Castel
153 Maggiore, Bologna, Italy) at 28 °C. Eluent A: Acetonitrile/H_2O 60:40, 10 mM ammonium formate, 0.1% FA;
154 eluent B: Isopropanol/Acetonitrile 90:10, 2 mM ammonium formate, 0.1% FA. All solvents were LC-MS grade.
155 The elution program consisted of a gradient from 20 to 40% B in 6.5 min, then to 50% B up to 13 min, reaching
156 90% B at min 16, holding for 1 min and returning back to 20% B in 1 min. A re-equilibration step of 5 mins was
157 included prior to each analysis. Flow rate was 0.3 mL/min. Samples were run in triplicates and the injection
158 volume was 10 µL; the column temperature was set at 40°C and the autosampler was maintained at 10°C. MS
159 analysis was performed on a Q Exactive Hybrid Quadrupole-Orbitrap mass spectrometer (Thermo Scientific,
160 San Jose, CA, USA) equipped with a HESI source. Source parameters were as follows: spray voltage positive
161 polarity 3.2 kV, negative polarity 3.0 kV, Capillary temperature 320 °C, S-lens RF level 55, Auxiliary gas
162 temperature 350 °C, Sheath gas flow rate 60, Auxiliary gas flow Rate 35. Full MS scans were acquired in the
163 range 200-1200 m/z at 70000 of mass resolution. For MS/MS analysis a data dependent ddMS2 Top10 method
164 was used; Mass Resolution was 17500, AGC Target 1e5, Acquisition Time 70ms. Mass fragmentation was
165 obtained with a stepped normalized energy (NCE) of 16-20 and 20-40 in positive and negative ionization mode,
166 respectively. A pool of in-house and commercial standard mix (SPLASH-Lipidomix, AvantiPolar Lipids) was used
167 as reference for MS/MS regioisomeric FA characterization. Raw LC-MS/MS data were processed with the
168 Xcalibur software (Thermo Scientific, version 3.1.66.10); lipid species were identified and quantified with the
169 support of LipidSearch software (Thermo Scientific, version 4.1.30). All data were manually double checked.

170

3. Results and Discussion

3.1 Sample preparation

Durum wheat cv. Svevo was selected for this study because it is a well characterized reference cultivar, widely used as a crossing parent worldwide. Grain samples were harvested at five developmental stages in the post-anthesis period, namely 5 (T1), 11 (T2), 16 (T3), 21 (T4) and 30 (T5) dpa, corresponding to partial kernel development (T1-T2), full kernel development (T3-T4) and grain maturation and desiccation (T5) stages. After lyophilization samples were extracted by a chloroform/methanol mixture according to a modified Blight and Dyer method to recover both starch and non-starch lipids.

3.2 HPTLC screening

A preliminary screening carried out by HPTLC (**Fig. S1**) clearly evidenced the progressive accumulation of TAG and a decrease of FFA in wheat kernels particularly evident at T5. TAG were detected already at T1 stage, albeit at very low amount. Few spots of unresolved polar lipids appeared at lower Rf.

3.3 GC-MS analysis

TAG were identified and quantified by capillary GC-MS at the different stages of kernel development. In agreement with HPTLC, TAG were detected already at T1 and progressively increased up to T5. In general, the profiles were dominated by TAG containing 54 acyl carbons (C54), followed by C52 and C56 TAG by abundance. Interestingly, the ratio of TAG groups at the early developmental stage (T1) was different, since C52 TAG were more abundant than C54 ones, whereas C56 TAG were undetectable (**Fig. S2**).

Independent GC-MS analysis of FFA as methyl esters (FAME) confirmed that at the initial stage the main FA were palmitic (C16:0) and oleic (C18:1) acids. Notably, the synthesis of polyunsaturated linoleic (C18:2n6) and linolenic (C18:3n-3) acids started being significant already from T2. These FA became prevalent in the T3/T4 filling stages, while they dropped down dramatically during the T5 period (**Fig. S3**). These results are in line with

195 the previous observations that the increased content of unsaturated FA was paralleled by the FFA decline
196 during grain maturation (Daftary and Pomeranz, 1965).
197
198 *3.4 UHPLC-Q Exactive MS/MS analysis*
199 An in-depth analysis of wheat lipidome was then performed using the high-resolution LC-MS Q Exactive
200 platform. Software-assisted lipid profiling allowed the unambiguous identification of overall 24 lipid classes and
201 190 main individual species. Interestingly, raw lipid profiling disclosed a complex pattern of polar lipids
202 occurring along with major TAG (**Fig. 1 and Fig S4**). Lipid compounds were identified and corresponding peak
203 areas compared by software-assisted analysis, exclusively on kernel dry weight basis.
204
205 *3.4.1 Triacylglycerols (TAG)*
206 Overall, 64 species of TAG were identified and characterized for their FA composition. The predominant groups
207 were C52 and C54, which exhibited an evident positive trend from T1 to T5 (**Fig. 2)**. A detailed investigation of
208 the FA composition revealed that the highest increment involved the species containing oleic and linoleic acids
209 (C54:3, C54:4, C54:5 and C54:6) followed by mixed C16/unsaturated C18 TAG (C52:2, C52:3 and C52:4) and to a
210 lesser extent by C56 series (C56:3, C56:4, C56:5) (**Table 1**). On the contrary, C42-C50 and odd FA-containing
211 TAG remained substantially unchanged or showed minor changes through the various maturation phases. TAG
212 were the most abundant and assorted class in terms of type and combination of FA on the three carbon
213 positions of glycerol. Furthermore, their constant increment from initial development to final desiccation stage
214 of wheat kernels is in agreement with their intrinsic role of storage reservoirs.
215
216 *3.4.2 Diacylglycerols (DAG)*
217 Diacylglycerols (DAG) as a class (**Fig. S4B and S5**) appeared early, already at T1, exhibited a sharp increase in
218 unsaturated species from T2 to T3, peaked at T4, after which they dropped at full kernel maturity. This class of
219 lipids plays a central biosynthetic role, being the building block for *de novo* formation of all membrane and

storage lipids in plants. Their decrease corresponds to a massive DAG-to-TAG biosynthetic conversion during the last stage (T5), when the entire lipid biosynthesis tends to converge into TAG accumulation. More in detail, the highest increment observed at the T3/T4 stages was recorded for the polyunsaturated FA-containing DAG (PUFA-DAG), i.e. DAG 16:0/18:2 and 18:2/18:2 and slightly lesser 18:1/18:2. Conversely, DAG analogs composed by palmitic and oleic acids maintain a basal level throughout kernel maturation. These latter species are synthesized *de novo* through the acylCoA/phosphatidic acid (PA) pathway (Kennedy pathway) and as precursors serve to the biosynthesis of polar and neutral glycerolipids containing C16:0 and C18:1 FA. The occurrence of PUFA-DAG analogs starting from T3 stage suggests the activation/prevalence at this period of other DAG biosynthetic pathways, including *de novo* DAG synthesis combined with phosphatidylcholine (PC)-FA modification and acyl editing and PC-derived DAG synthesis (Bates and Browse, 2012). In fact, C18:1 FA is desaturated to C18:2 and C18:3 on PC so that PUFA-PC can accumulate and in part be converted into PUFA-DAG, which in turn represent the committed precursors of PUFA-TAG.

3.4.3 Phospholipids (PL)

The most represented PC species was the 16:0/18:2 derivative (**Table 2**). However, PC 18:2/18:2 showed a continuous increase up to final stage T5. This finding further supports the central role of PC 18:2/18:2 species also in TAG biosynthesis. On the other side, the PUFA enrichment observed in phosphatidylethanolamines (PE), phosphatidylinositols (PI) and phosphatidylglycerols (PG) during grain maturation (**Fig. S4B**) can be ascribed to the utilization of PUFA-DAG for the formation of all these lipids. Together with DAG, the other key precursor for *de novo* biosynthesis of all lipid classes is PA, typically in the form of PA 16:0/18:1 or 18:1/18:1. Indeed, in wheat samples here examined PA occurred mainly as 16:0/18:2 and 18:2/18:2 molecular species, thus suggesting a biosynthetic process involving PC with unsaturated FA (i.e. PC 16:0/18:2 and 18:2/18:2) as acyl donor for the consecutive acylation steps of glycerol-3-phospate and lysophosphatidic acid (LPA), finally leading to a DAG pool rich in PC-modified FA for TAG synthesis (Bates and Browse, 2012) (**Table 2**). Hence, it appears straightforward the involvement of these PA as key intermediates in the biosynthesis of polyunsaturated lipids,

245 including TAG. An additional intriguing possibility is that PA may act as signaling molecules, produced under
246 certain stress/stimuli (Wang et al., 2006). In fact, PA have been implicated in various plant processes which
247 include responses to abiotic and biotic stresses (drought, chilling, nutrient starvation, ROS, wounding and
248 microbial elicitation) and involvement in specific steps of growth and development, such as seed germination,
249 seed aging, leaf senescence, root hair patterning, root growth, pollen germination, and pollen tube growth.
250 However, a putative signaling role of PA in grain maturation has been never reported so far and it would
251 deserve further investigation.
252 All PL, including PE, PG, PI showed a similar T3/T4 peak of relative abundance as monitored in LC-MS profiles
253 (**Fig. S6**). Regiochemistry of PL was assigned according to previous interpretative studies (Hsu and Turk, 2009)
254 and confirmed by a commercial standard mix run in our conditions on ESI-Q Exactive platform. The general
255 strategy for PC, PE, PG and PI identification by MS/MS is based on the preferred loss of both carboxylate and
256 ketene ions from position *sn*-2 of the glycerol backbone. Hence, the peak intensity of the resulting [M-
257 $R_2CH=C=O]^-$ and R_2COO^- product ions are much higher than $[M-R_1CH=C=O]^-$ and R_1COO^- ions in product spectra of
258 either $[M-H]^-$ or $[M+HCOO]^-$ adducts, thus allowing to assign FA position on the glycerol backbone (**Table 2**).
259 Conversely, while fragmentation of PA ion at *sn*-2 is still favored, generating major loss of carboxylate with
260 corresponding $[M-H-R_2COOH]^-$>$[M-H-R_1COOH]^-$, successive CID fragmentations of these intermediate products
261 favor further loss of carboxylate from *sn*-1 of $[M-H-R_2COOH]^-$ ion following a charge-driven process; in these
262 conditions, R_1COO^- ion net intensity resulted higher than R_2COO^- in product spectra, which is the opposite of
263 what observed with all the other PL. Therefore, based on an in-depth interpretation of all MS/MS data,
264 regiochemical distribution of FA was established for each identified PL species; regiochemical analysis allowed
265 to detect two couples of regioisomeric species, eluting at slightly different retention time (t_R) as reported in
266 **Table 2**, namely PA 36:5 (18:3/18:2 and 18:2/18:3) and PG 36:5 (18:2/18:3 and 18:3/18:2). All data were
267 indicative of a eukaryotic biosynthetic pathway for all glycerophospholipid classes. In fact, C18 acids were
268 found at both *sn*-1 and *sn*-2 glycerol positions, while C16:0 was exclusively located at the *sn*-1 position.

269 Apart from PA, whose composition and involvement in biosynthetic processes has been previously discussed,
270 PC, PE, and PI showed prevalence of 16:0/18:1 species at the beginning (48.2-90.8 %) replaced by 16:0/18:2
271 and 18:2/18:2 species in later stages. In line with their plastidial biosynthetic origin, PG showed initially >67% of
272 C16:0/16:0 species, supplanted by PUFA C18 species over time.
273
274 *3.4.4 Lysophospholipids (LPL)*
275 FA composition of lysophospholipids (LPA, LPC, LPE and LPG, **Fig. S7**) reflected the total natural FA abundance
276 along with the observed variation in unsaturation of C18 FA during grain growth. However, they started to be
277 significant a few days post anthesis, since they were detected only in traces in T1 samples. Lysolipids including
278 minor monoacylglycerols (MAG) are considered "true" starch lipids, while full acylated lipids are non-starch
279 lipids, occurring in endosperm, aleurone and germ. Previous studies have excluded that they are simple
280 degradative forms of corresponding acylated lipids due to extraction artefacts. Thus, their biosynthesis is
281 supposed to be independently regulated from that of the corresponding PL. On the other hand, lysolipids are
282 located inside starch granules, tightly associated with amylose helix, so that their biosynthesis likely is
283 synchronous with starch formation. Indeed, previous studies carried on the same durum wheat cultivar
284 evidenced that expression of starch biosynthetic enzymes started at T2 and peaked at T3/T4 stages, which is in
285 agreement with major levels of lysolipids in our extract profiles (Arena et al., 2017). Coherently, starch granules
286 were detected by light microscopy in grain-cross section from 15 dpa in the endosperm cells, which
287 corresponds to T3/T4 in our harvested samples (Guillon et al., 2012).
288
289 *3.4.5 Galactolipids (GL)*
290 Digalactosylglycerols (DGDG) and monogalactosylglycerols (MGDG) (**Table 3 and Fig.S8**) were dominated by
291 C18:2 FA containing species, which registered the highest level in T5. Evolution of GL through T1-T5 showed
292 Gaussian profiles resembling those of PL. In fact, DGDG and MGDG species containing C16:0 and C18:1 FA,
293 poorly represented in absolute levels in T1, account for 78.0 % and 89.1%, respectively, in relative terms, while

294 at T3 stage they dropped at 50.6% and 21.9%, respectively. In contrast, 18:2 containing individual species rose
295 at 46.7% for DGDG and 66.0 % for MGDG at T3, starting from T1 values of 22.0% and 5.8%, respectively. The
296 level of C18:2/18:2 species in both MGDG and DGDG continuously increased up to T5, paralleling the trend of
297 C18:2-containing TAG, in agreement with previous findings (Weber, 1970). In T5, species composed by
298 18:2/18:2 represented 47.3% of DGDG and 61.9% of MGDG.
299 Regiochemical analysis was carried out on samples processed according to our previous studies (Cutignano et
300 al., 2016) and was based on the general behavior of sodium adducts of glycoglycerolipids to produce
301 preferentially fragmentation of acyl chain at the glycerol *sn*-1 position. Extensive MS/MS data interpretation
302 revealed that both DGDG and MGDG were mainly synthesized by the eukaryotic pathway.
303
304 *3.4.6 Sphingolipids (SP)*
305 Sphingolipids (SP), i.e. ceramides (Cer) and glucosylceramides (GlcCer) (**Fig. 1**), are evenly distributed in all parts
306 of wheat kernel (Geng et al., 2015). By our LC-MS analyses, 30 SP species were characterized (**Table 4 and Fig.**
307 **S9**). The FA composition of these minor lipids encompasses mainly saturated, long chain FA, even but not
308 exclusively in oxygenated form, in part contrasting with recent reports from wheat (Geng et al., 2015; Zhu et
309 al., 2013). Compared with other previous reports (Fujino and Ohnishi, 1983), we found some differences in SP
310 composition. In the 20 molecular species of ceramides detected, the most abundant FA were C16:0, C24:0, also
311 oxygenated, along with C18:1 and C24:1. Differently from ceramide composition recently reported in soft
312 wheat (Geng et al., 2015), in durum wheat here analyzed sphingoid long chain base (LCB) mainly occurred as
313 phytosphingosine (t18:0) along with sphingosine (d18:1), with minor contribution from sphingadienine (d18:2),
314 sphinganine (d18:0), and d20:1 sphingoid LCB. The main species of Cer resulted t18:0/24:0, t18:0/24:1 and
315 d18:1/24:0+O. Notably, in our LC-MS conditions ceramides of the same lipid group can be easily distinguished
316 as for LCB and FA composition based on both Rt and MS/MS fragments (**Table 4**). For example, as showed in
317 **Table 4**, three ions belonging to the group d42:1+O have been detected at t_R=9.51, 9.59 and 9.65 min for which
318 the same molecular formula $C_{42}H_{83}O_4N$ (calculated *m/z* 666.6395) can be inferred by high accuracy

measurement of the corresponding observed ion masses. Detailed analysis of MS/MS product ions allowed to distinguish the lipid species resulting from the combination of three different LCB and FA, namely: Cer(t18:0/24:1), Cer(d18:1+O/24:0) and Cer(d18:1/24:0+O), respectively. Ceramides could be revealed already at T1 stage and at an appreciable level in comparison with successive stages. On the contrary, biosynthesis of glycosylated forms appeared more active at later stages (T3 and T4). This is an interesting point that has been never discussed before.

Glycosylceramides (GlcCer) showed lower chemical diversity compared to Cer. The structural identity of the monosaccharide residue was not investigated here, thus we generically refer to all of them as monoglycosyl derivatives. However, in plants the monosaccharide unit is typically represented by D-glucopyranose in β-linkage to the C-1 hydroxyl group of the ceramide backbone. Occasionally, mannose has been found linked to the sphingoid LCB. Overall, 10 species were identified, one of which was predominant, specifically that containing d18:1/C16:0+O as the ceramide portion. Minor species typically showed the occurrence of monounsaturated or mono-oxygenated saturated FA (20:0, 22:0 and 24:0) that do not have a counterpart in the ceramide pool. In general, it seems that there is no direct correspondence between Cer and glycosylated analogs, since major GlcCer derived from preferential glycosylation of less abundant Cer species. This aspect has been evidenced in previous papers (Fujino and Ohnishi, 1983) and suggests the origin of Cer and GlcCer from biosynthetic pathways probably fueling two independent pools with different functions. In fact, in contrast with main Cer species, the highest relative abundance of Cer d18:1/C16:0+O in T3/T4 stages matches the highest peaks of the corresponding glycosylated products at the same stages (**Fig S9**). Indeed, plant sphingolipids are not only structural components of the plasma membrane and other endocellular membranes, but they also act as signaling molecules in response to biotic and abiotic stresses, despite this role is far for being properly investigated (Ali et al., 2018).

SP profiling deserves an additional comment since none of the previous works took into consideration the biosynthetic evolution of this class of lipids. Considering the total ion current of both total lipids and each individual species, the trend is basically the same as the other lipids. However, it is quite worth noting that Cer

344 are actively synthesized in an appreciable amount soon after anthesis together with TAG, DAG and PA. This
345 may suggest a specific role of SP during the early phase of grain development; in effect, while DAG and PA are
346 clearly correlated to biosynthesis of TAG, the main lipids, Cer and other SP might function as signaling
347 molecules and perform regulatory roles in a series of biosynthetic and physiological processes including cell-
348 wall formation (Lynch and Dunn, 2004) and cell type differentiation (Msanne et al., 2015). In effect, during the
349 initial stage of kernel development, cell division is very high to allow morphogenesis and organogenesis, thus
350 supporting a plausible involvement of SP as metabolic signals. However, determining the biological functions of
351 SP is challenging since each class, including Cer, GlcCer and sphingoid LCB plays a specific role either on its own
352 or in homoeostasis with the others, being SP metabolites continuously converted into each other via
353 biosynthetic and degradative pathways (Pata et al., 2010).
354
355 *3.4.7 Phytosterols*
356 Wheat phytosterols represent an additional variegate class of structurally related compounds (Zhu and
357 Nyström, 2019). Sitosterol is the most abundant component of wheat phytosterols, accounting for 51-54% of
358 total sterols with a constant proportion among the wheat varieties (Nurmi et al., 2008). These compounds
359 occur also as steryl glycosides formed through a β-glycosidic linkage between the C1 position of several
360 possible monosaccharides (most frequently D-glucopyranose) and the C3 position of sterol mojety. In this
361 study, sterols were detected as fatty acyl sitosteryl glycosides (AGlcSiE) with main FA, i.e. 16:0, 18:2 and 18:3
362 esterifying hydroxyl group at C6 of the monosaccharide unit (**Fig. 1)**. These were minor compounds, found at
363 comparable amounts during all stages of grain filling although the chemical composition varied throughout the
364 growing stages, with a progressive increase of the C18:2 derivative (**Fig. S10**). Despite extensive research on the
365 occurrence of phytosterol esters in plants, acyl steryl glycosides are poorly characterized concerning structural
366 variety and biological function (Ferrer et al., 2017). However, in consideration of their low abundance, they are
367 expected to not impact technological and functional traits of wheat flour and dough. Furthermore, glycosyl
368 phytosterols might be scarcely retained in the cooked pasta, leaching in cooking water due to a certain

369 solubility. On the other hand, the broad class of wheat phytosterols has been rather investigated for their
370 possible nutritional relevance (Nurmi et al., 2008).
371
372 *3.4.8 Other lipids*
373 Finally, the lipidome of durum wheat also includes a series of additional compounds, such as waxes,
374 tocochromanols, carotenoids (e.g. xanthophylls), free sterols, terpene alcohols and alkylresorcinols, which for
375 the most have been already inventoried through dedicated workflows of purification and analysis (Geng et al.,
376 2015; Lafiandra et al., 2012). Thus, these minor compounds have been not the focus of the present study.
377

378 4. Conclusions

379 This study represents the first lipidome characterization of durum wheat during grain maturation, over a period
380 covering 5-30 dpa that is from embryo development to full maturation. The opportunity to apply advanced
381 high-resolution MS methodologies allowed to monitor the evolution of individual lipid classes at the molecular
382 level over five key developing stages. The progressive increase in unsaturation degree of FA acyl chains during
383 grain maturation has been described since long. On the other hand, here for the first time the trend in FA
384 composition for each of the main lipid classes and the dynamics ruling the relative balance of lipid classes have
385 been inferred at the key stages of grain filling by UHPLC-HRESI-MS/MS analysis. A general trend shared by all
386 lipid classes is the prevalence of palmitate and oleate-based lipids during the early developmental stages (T1
387 and T2), with an increment of linoleate and linolenate- containing species during the grain filling and
388 maturation stages (T3-T5). Except for TAG, the metabolic activation of lipid biosynthesis begins between T2 and
389 T3 stages, i.e. at the turn of two weeks (11-16 dpa), lasting until the dough stage. The biosynthesis of the
390 different lipid classes and, within each class, of specific components follows a seed maturation program that
391 can be explained only in part in the light of the current defined metabolic pathways. In line with fragmentary
392 data available for soft wheat and other cereals (i.e. maize) (Stokes et al., 1986; Weber, 1970, 1969), the current

findings provide an in-depth view into lipid metabolism during the process of grain filling and maturation, still poorly studied from a biochemical standpoint. The preliminary nature of the present study, which could not rely on biological replicates for appropriate statistical analysis of LC-MS data, implies some limitations for the assessment of the reported values. At this stage, the aim and the implications of the research were to propose an in-depth view into lipid metabolism during the process of grain maturation, still poorly investigated from a (bio)chemical point of view. Follow-up of this study with other durum wheat cultivars will also be needed to generalize our results. Furthermore, several metabolic and functional features of lipids await to be defined, such as the involvement of key intermediates (i.e. PUFA-PC and -PA) in the possible pathways leading to (poly)unsaturated TAG and the physiological role of bioactive lipids, such as sphingolipids. The combination of lipidomic with partly available genomic, transcriptional, metabolomic and proteomic data, enables systems biology approaches to assist breeding, improve agronomical practices and enhance grain quality. The global biomolecular and metabolic perspective could be conveniently exploited in the next future for engineered modulation of specific lipid components, such as dietary essential FA or bioactive sphingolipids in desirable larger quantity. In addition, the knowledge of the differences in lipid compositions of wheat cultivars may make virtually possible to produce flours or recover bran and/or germ oil with purposely modified lipid compositions suited for different end uses.

Acknowledgements

This work was partly supported by a grant from MIUR-CNR: Progetto Bandiera “InterOmics”: *Sviluppo di una piattaforma integrata per l’applicazione delle scienze “omiche” alla definizione dei biomarcatori e profili diagnostici, predittivi, e teranostici*.

References

Ali, U., Li, H., Wang, X., Guo, L., 2018. Emerging roles of sphingolipid signaling in plant response to biotic and

abiotic stresses. Mol. Plant 11, 1328–1343.

Arena, S., D'Ambrosio, C., Vitale, M., Mazzeo, F., Mamone, G., Di Stasio, L., Maccaferri, M., Curci, P.L., Sonnante, G., Zambrano, N., Scaloni, A., 2017. Differential representation of albumins and globulins during grain development in durum wheat and its possible functional consequences. J. Proteomics 162, 86–98.

Barron, C., Surget, A., Rouau, X., 2007. Relative amounts of tissues in mature wheat (Triticum aestivum L.) grain and their carbohydrate and phenolic acid composition. J. Cereal Sci. 45, 88–96.

Cutignano, A., Luongo, E., Nuzzo, G., Pagano, D., Manzo, E., Sardo, A., Fontana, A., 2016. Profiling of complex lipids in marine microalgae by UHPLC/tandem mass spectrometry. Algal Res. 17, 348-358.

Daftary, R.D., Pomeranz, Y., 1965. Changes in lipid composition in maturing wheat. J. Food Sci. 30, 577–582.

Ferrer, A., Altabella, T., Boronat, A., 2017. Emerging roles for conjugated sterols in plants. Prog. Lipid Res. 67, 27–37.

Fujino, Y., Ohnishi, M., 1983. Sphingolipids in wheat grain. J. Cereal Sci. 1, 159–168.

Geng, P., Harnly, J.M., Chen, P., 2015. Differentiation of Whole Grain from Refined Wheat (T. aestivum) Flour Using Lipid Profile of Wheat Bran, Germ, and Endosperm with UHPLC-HRAM Mass Spectrometry. J. Agric. Food Chem. 63, 6189–6211.

González-Thuillier, I., Salt, L., Chope, G., Penson, S., Skeggs, P., Tosi, P., Powers, S.J., Ward, J.L., Wilde, P., Shewry, P.R., Haslam, R.P., 2015. Dis$_{tr}$ibution of Lipids in the Grain of Wheat (cv. Hereward) Determined by Lipidomic Analysis of Milling and Pearling Fractions. J. Agric. Food Chem. 63, 10705–10716.

Guillon, F., Larré, C., Petipas, F., Berger, A., Moussawi, J., Rogniaux, H., Santoni, A., Saulnier, L., Jamme, F., Miquel, M., Lepiniec, L., Dubreucq, B., 2012. A comprehensive overview of grain development in Brachypodium distachyon variety Bd21. J. Exp. Bot. 63, 739–755.

Hsu, F.F., Turk, J., 2009. Electrospray ionization with low-energy collisionally activated dissociation tandem mass spectrometry of glycerophospholipids: Mechanisms of fragmentation and structural characterization. J. Chromatogr. B Anal. Technol. Biomed. Life Sci. 877, 2673–2695.

442 Klopfenstein, W.E., Pomeranz, Y., 1968. Fatty acids in lipids of maturing wheat. Lipids 3, 557–560.
443 Lafiandra, D., Masci, S., Sissons, M., Dornez, E., Delcour, J.A., Courtin, C.M., Caboni, M.F., 2012. Kernel
444 Components of Technological Value in Durum Wheat Chemistry and Technology: Second Edition. AACC
445 International, Inc., pp. 85-124.
446 Liu, K.S., 2011. Comparison of Lipid Content and Fatty Acid Composition and Their Distribution within Seeds of
447 5 Small Grain Species. J. Food Sci. 76, C334–C342.
448 Lynch, D. V, Dunn, T.M., 2004. An introduction to plant sphingolipids and a review of recent advances in
449 understanding their metabolism and function. New Phytol. 161, 677–702.
450 Maccaferri, M., Harris, N.S., Twardziok, S.O., Pasam, R.K., Gundlach, H., Spannagl, M., Ormanbekova, D., Lux, T.,
451 Prade, V.M., Milner, S.G., Himmelbach, A., Mascher, M., Bagnaresi, P., Faccioli, P., Cozzi, P., Lauria, M.,
452 Lazzari, B., Stella, A., Manconi, A., Gnocchi, M., Moscatelli, M., Avni, R., Deek, J., Biyiklioglu, S., Frascaroli,
453 E., Corneti, S., Salvi, S., Sonnante, G., Desiderio, F., Marè, C., Crosatti, C., Mica, E., Özkan, H., Kilian, B., De
454 Vita, P., Marone, D., Joukhadar, R., Mazzucotelli, E., Nigro, D., Gadaleta, A., Chao, S., Faris, J.D., Melo,
455 A.T.O., Pumphrey, M., Pecchioni, N., Milanesi, L., Wiebe, K., Ens, J., MacLachlan, R.P., Clarke, J.M., Sharpe,
456 A.G., Koh, C.S., Liang, K.Y.H., Taylor, G.J., Knox, R., Budak, H., Mastrangelo, A.M., Xu, S.S., Stein, N., Hale, I.,
457 Distelfeld, A., Hayden, M.J., Tuberosa, R., Walkowiak, S., Mayer, K.F.X., Ceriotti, A., Pozniak, C.J., Cattivelli,
458 L., 2019. Durum wheat genome highlights past domestication signatures and future improvement targets.
459 Nat. Genet. 51, 885–895.
460 MacRitchie, F., 1977. Flour lipids and their effects in baking. J. Sci. Food Agric. 28, 53–58.
461 Mahmoud, A.A., Mohdaly, A.A.A., Elneairy, N.A.A., 2015. Wheat Germ: An Overview on Nutritional Value,
462 Antioxidant Potential and Antibacterial Characteristics. Food Nutr. Sci. 06, 265–277.
463 Mazzeo, M.F., Di Stasio, L., D'Ambrosio, C., Arena, S., Scaloni, A., Corneti, S., Ceriotti, A., Tuberosa, R., Siciliano,
464 R.A., Picariello, G., Mamone, G., 2017. Identification of Early Represented Gluten Proteins during Durum
465 Wheat Grain Development. J. Agric. Food Chem. 65, 3242–3250.
466 Morrison, W.R., 1994. Wheat lipids: structure and functionality. Wheat 128–142.

Msanne, J., Chen, M., Luttgeharm, K.D., Bradley, A.M., Mays, E.S., Paper, J.M., Boyle, D.L., Cahoon, R.E., Schrick, K., Cahoon, E.B., 2015. Glucosylceramides are critical for cell-type differentiation and organogenesis, but not for cell viability in Arabidopsis. Plant J. 84, 188–201.

Narducci, V., Finotti, E., Galli, V., Carcea, M., 2019. Lipids and fatty acids in Italian durum wheat (Triticum Durum Desf.) cultivars. Foods 8, 1–9.

Nurmi, T., Nyström, L., Edelmann, M., Lampi, A.-M., Piironen, V., 2008. Phytosterols in Wheat Genotypes in the HEALTHGRAIN Diversity Screen. J. Agric. Food Chem. 56, 9710–9715.

Pata, M.O., Hannun, Y.A., Ng, C.K.Y., 2010. Plant sphingolipids: Decoding the enigma of the Sphinx. New Phytol. 185, 611–630.

Qin, H., Ma, D., Huang, X., Zhang, J., Sun, W., Hou, G., Wang, C., Guo, T., 2019. Accumulation of glycolipids in wheat grain and their role in hardness during grain development. Crop J. 7, 19–29.

Stokes, D.N., Galliard, T., Harwood, J.L., 1986. Changes in the lipid composition of developing wheat seeds. Phytochemistry 25, 811–815.

Wang, X., Devaiah, S.P., Zhang, W., Welti, R., 2006. Signaling functions of phosphatidic acid. Prog. Lipid Res. 45, 250–278.

Weber, E.J., 1969. Lipids of maturing grain of corn (Zea mays L.): - I. Changes in lipid classes and fatty acid composition. J. Am. Oil Chem. Soc. 46, 485–488.

Weber, E.J., 1970. Lipids of maturing grain of corn (Zea mays L.): - II. Changes in polar lipids. J. Am. Oil Chem. Soc. 47, 340–343.

Wetzel, D.L., Boatwright, M.D., Fritz, A.K., 2014. Tandem mass spectrometric determination of glycolipids in wheat endosperm: A new tool for breeders to rank and select early seed generations. JAOCS, J. Am. Oil Chem. Soc. 91, 1849–1855.

490 **Table 1.** Identification, characterization and relative abundance of TAG species in wheat kernel across T1-T5
491 maturation stages. Values (%) are average of three replicates. Relative standard deviation was lower than 10 %
492 in all cases and was not reported. All species were detected as NH_4^+ adducts.

FA Group Key	Lipid Molecular Species	Base t_R (min)	Formula	Obs Mass	Calc *m/z*	T1	T2	T3 %	T4	T5
42:0	TG(16:0/12:0/14:0)	15,91	C45 H86 O6	740.6768	740.6763	1,30	1,17	0,93	0,78	0,68
43:0	TG(15:0/14:0/14:0)	16,00	C46 H88 O6	754.6926	754.6919	1,43	1,21	1,08	0,93	0,63
43:1	TG(16:1/13:0/14:0)	15,91	C46 H86 O6	782.7234	782.7232	0,82	0,72	0,59	0,39	0,30
44:0	TG(16:0/14:0/14:0)	16,17	C47 H90 O6	768.7079	768.7076	3,10	2,56	2,39	2,05	1,47
44:1	TG(16:1/14:0/14:0)	16,08	C47 H88 O6	766.6921	766.6919	1,96	1,68	1,49	1,34	0,99
44:2	TG(16:1/14:0/14:1)	15,99	C47 H86 O6	764.6767	764.6763	0,80	0,66	0,61	0,53	0,34
45:0	TG(15:0/14:0/16:0)	16,25	C48 H92 O6	782.7234	782.7232	3,49	3,21	2,66	2,47	1,77
45:1	TG(15:0/14:0/16:1)	16,20	C48 H90 O6	780.7081	780.7076	2,42	2,15	1,74	1,66	1,20
45:2	TG(15:0/14:1/16:1)	16,11	C48 H88 O6	778.6931	778.6919	0,91	0,57	0,72	0,62	0,43
46:0	TG(16:0/14:0/16:0)	16,37	C49 H94 O6	796.7392	796.7389	6,42	5,90	4,59	4,13	3,40
46:1	TG(16:0/14:0/16:1)	16,33	C49 H92 O6	794.7238	794.7232	4,64	4,25	3,56	3,06	2,36
46:2	TG(16:1/14:0/16:1)	16,26	C49 H90 O6	792.7086	792.7076	2,47	2,26	1,80	1,55	1,35
47:0	TG(15:0/16:0/16:0)	16,46	C50 H96 O6	810.7543	810.7545	4,48	4,39	3,59	3,10	2,36
47:1	TG(15:0/16:0/16:1)	16,41	C50 H94 O6	808.7393	808.7389	4,80	4,48	3,41	3,03	2,58
47:2	TG(15:0/16:1/16:1)	16,36	C50 H92 O6	806.7242	806.7232	2,38	2,24	1,75	1,53	1,29
48:0	TG(16:0/16:0/16:0)	16,55	C51 H98 O6	824.7692	824.7702	5,13	6,06	4,57	3,93	2,69
48:1	TG(16:0/16:0/16:1)	16,51	C51 H96 O6	822.7545	822.7545	6,01	5,80	4,84	4,06	3,08
48:2	TG(16:0/16:1/16:1)	16,47	C51 H94 O6	820.7399	820.7389	4,27	4,06	3,29	2,78	2,20
48:3	TG(16:1/16:1/16:1)	16,41	C51 H92 O6	818.7240	818.7232	1,30	1,25	0,95	0,90	0,69
49:1	TG(15:0/16:0/18:1)	16,58	C52 H98 O6	836.7707	836.7702	3,54	3,36	2,65	2,20	1,66

49:2	TG(16:0/16:1/17:1)	16,54	C52 H96 O6	834.7549	834.7545	2,77	2,54	1,92	1,69	1,48
49:3	TG(16:1/16:1/17:1)	16,48	C52 H94 O6	832.7389	832.7389	0,75	0,73	0,57	0,49	0,44
50:1	TG(16:0/16:0/18:1)	16,66	C53 H100 O6	850.7863	850.7858	4,12	3,67	3,35	2,96	2,65
50:2	TG(16:0/16:1/18:1)	16,61	C53 H98 O6	848.7712	848.7701	4,33	4,22	4,25	5,27	5,10
50:3	TG(16:1/16:1/18:1)	16,56	C53 H96 O6	846.7561	846.7545	1,85	1,88	1,56	1,50	1,25
51:1	TG(16:0/17:0/18:1)	16,74	C54 H102 O6	864.8019	864.8015	1,45	1,41	0,97	0,77	0,64
51:2	TG(16:1/17:0/18:1)	16,71	C54 H100 O6	862.7870	862.7858	1,51	1,56	1,09	0,93	0,71
51:3	TG(16:1/17:1/18:1)	16,66	C54 H98 O6	860.7711	860.7702	0,75	0,72	0,56	0,45	0,40
52:1	TG(18:0/16:0/18:1)	16,78	C55 H104 O6	878.8139	878.8171	1,34	1,34	0,98	0,98	0,83
52:2	TG(16:0/18:1/18:1)	16,77	C55 H102 O6	876.8013	876.8015	2,60	2,66	2,65	2,97	3,55
52:3	TG(16:0/18:1/18:2)	16,71	C55 H100 O6	874.7865	874.7858	1,79	2,05	3,66	4,98	6,18
52:4	TG(16:0/18:2/18:2)	16,65	C55 H98 O6	872.7703	872.7702	0,80	1,44	5,72	8,72	9,50
52:5	TG(16:0/18:2/18:3)	16,59	C55 H96 O6	870.7542	870.7545	0,17	0,76	2,31	2,52	2,12
52:6	TG(16:0/18:3/18:3)	16,51	C55 H94 O6	868.7379	868.7389	0,08	0,36	0,50	0,26	0,17
53:0	TG(16:0/14:0/23:0)	16,89	C56 H108 O6	894.8488	894.8484	0,51	0,55	0,41	0,31	0,24
53:2	TG(17:0/18:1/18:1)	16,83	C56 H104 O6	890.8178	890.8171	0,54	0,51	0,36	0,30	0,28
54:0	TG(18:0/16:0/20:0)	16,95	C57 H110 O6	908.8634	908.8641	1,01	1,01	0,72	0,55	0,48
54:2	TG(16:0/18:1/20:1)	16,90	C57 H106 O6	904.8296	904.8328	0,98	0,99	0,89	0,85	1,04
54:3	TG(18:1/18:1/18:1)	16,86	C57 H104 O6	902.8170	902.8171	1,92	2,15	2,13	1,82	3,74
54:4	TG(18:1/18:1/18:2)	16,82	C57 H102 O6	900.8015	900.8015	0,74	1,17	2,38	2,43	5,13
54:5	TG(18:1/18:2/18:2)	16,77	C57 H100 O6	898.7859	898.7858	0,52	0,94	3,42	4,78	7,35
54:6	TG(18:2/18:2/18:2)	16,72	C57 H98 O6	896.7715	896.7702	0,31	0,97	3,96	5,29	7,04
54:7	TG(18:3/18:2/18:2)	16,65	C57 H96 O6	894.7540	894.7545	0,10	0,60	1,80	2,00	1,81
54:8	TG(18:3/18:2/18:3)	16,59	C57 H94 O6	892.7389	892.7389	0,02	0,34	0,47	0,32	0,26
55:0	TG(25:0/14:0/16:0)	16,98	C58 H112 O6	922.8790	922.8797	0,69	0,67	0,47	0,46	0,42
55:1	TG(16:0/16:1/23:0)	16,98	C58 H110 O6	920.8638	920.8641	0,50	0,54	0,41	0,33	0,31

55:2	TG(16:1/16:1/23:0)	16,97	C58 H108 O6	918.8487	918.8484	0,27	0,22	0,18	0,17	0,15
56:0	TG(16:0/16:0/24:0)	17,03	C59 H114 O6	936.8948	936.8954	0,79	0,85	0,57	0,50	0,50
56:1	TG(16:0/16:1/24:0)	17,02	C59 H112 O6	934.8795	934.8797	0,78	0,75	0,51	0,44	0,42
56:2	TG(16:1/18:1/22:0)	17,01	C59 H110 O6	932.8639	932.8641	0,43	0,44	0,37	0,37	0,36
56:3	TG(20:1/18:1/18:1)	16,97	C59 H108 O6	930.8471	930.8484	0,19	0,23	0,29	0,30	0,41
56:4	TG(20:1/18:1/18:2)	16,94	C59 H106 O6	928.8330	928.8328	0,12	0,16	0,24	0,32	0,51
56:5	TG(20:1/18:2/18:2)	16,90	C59 H104 O6	926.8159	926.8171	0,12	0,12	0,28	0,31	0,67
57:0	TG(25:0/16:0/16:0)	17,06	C60 H116 O6	950.9097	950.9110	0,63	0,58	0,48	0,38	0,37
57:1	TG(25:0/16:0/16:1)	17,06	C60 H114 O6	948.8954	948.8954	0,54	0,52	0,44	0,35	0,33
57:2	TG(16:1/18:1/23:0)	17,05	C60 H112 O6	946.8793	946.8797	0,30	0,25	0,22	0,20	0,17
58:1	TG(16:0/18:1/24:0)	17,10	C61 H116 O6	962.9100	962.9110	0,49	0,56	0,41	0,40	0,33
58:2	TG(16:1/18:1/24:0)	17,09	C61 H114 O6	960.8955	960.8954	0,37	0,40	0,31	0,31	0,29
58:3	TG(16:1/18:1/24:1)	17,05	C61 H112 O6	958.8770	958.8797	0,11	0,12	0,14	0,16	0,16
59:1	TG(25:0/16:0/18:1)	17,13	C62 H118 O6	976.9255	976.9267	0,28	0,28	0,22	0,22	0,18
59:2	TG(25:0/16:1/18:1)	17,13	C62 H116 O6	974.9106	974.9110	0,22	0,22	0,19	0,15	0,14
60:1	TG(26:0/16:0/18:1)	17,18	C63 H120 O6	990.9407	990.9423	0,26	0,24	0,21	0,18	0,17
60:2	TG(26:0/16:1/18:1)	17,17	C63 H118 O6	988.9262	988.9267	0,22	0,22	0,18	0,19	0,16
60:3	TG(18:1/18:2/24:0)	17,15	C63 H116 O6	986.9091	986.9110	0,08	0,10	0,08	0,08	0,09

493

494

495 **Table 2.** Identification and relative abundance of PL species within each subclass (PA, PC, PE, PG and PI) in
496 wheat kernel across T1-T5 maturation stages. Regiochemistry *sn*-1/*sn*-2 is indicated. Values (%) are means of
497 three replicates. Relative standard deviation was lower than 10 % in all cases and is not reported.
498

FA Group Key	Lipid Molecular Species	Base t_R (min)	Formula	Ion adduct	Obs mass	Calc *m/z*	T1	T2	T3	T4	T5
									%		
34:2	PA(16:0/18:2)	6,30	C37 H69 O8 P	M-H$^-$	671.4665	671.4657	58,35	42,95	44,87	50,50	48,50
34:3	PA(16:0/18:3)	5,86	C37 H67 O8 P	M-H$^-$	669.4519	669.4501	12,77	16,86	12,88	12,97	9,12
36:4	PA(18:2/18:2)	6,06	C39 H69 O8 P	M-H$^-$	695.4656	695.4657	22,41	27,41	32,37	31,62	37,69
36:5	PA(18:3/18:2)[a]	5,67	C39 H67 O8 P	M-H$^-$	693.4518	693.4501	6,48	12,78	9,88	4,91	4,68
36:5	PA(18:2/18:3)[a]	5,94	C39 H67 O8 P	M-H$^-$	693.4522	693.4501					
34.1	PC(16:0/18:1)[c]	7,09	C42 H82 N O8 P	M+H$^+$	760.5855	760.5850	48,17	28,90	13,54	8,56	9,52
				M+HCOO$^-$	804.5781	804.5760					
34:2	PC(16:0/18:2)	6,51	C42 H80 N O8 P	M+H$^+$	758.5708	758.5694	21,29	47,09	62,59	65,13	46,87
				M+HCOO$^-$	802.5625	802.5604					
36:2	PC(18:1/18:1)	7,66	C44 H84 N O8 P	M+HCOO$^-$	830.5937	830.5917	29,19	6,57	4,12	3,36	8,27
36:3	PC(18:1/18:2)	7,06	C44 H82 N O8 P	M+H$^+$	784.5857	784.5851	0,94	8,61	6,16	4,75	8,61
				M+HCOO$^-$	828.5789	828.5760					
36:4	PC(18:2/18:2)	6,45	C44 H80 N O8 P	M+HCOO$^-$	826.5615	826.5604	0,42	8,83	13,58	18,20	26,72
34:1	PE(16:0/18:1)	6,82	C39 H76 N O8 P	M-H$^-$	716.5247	716.5236	90,82	35,95	13,52	15,58	39,12
34:2	PE(16:0/18:2)	6,24	C39 H74 N O8 P	M-H$^-$	714.5091	714.5079	0,34	25,11	33,54	27,86	17,52
34:3	PE(16:0/18:3)	5,78	C39 H72 N O8 P	M-H$^-$	712.4938	712.4923	0,01	6,98	4,05	2,21	1,00
36:2	PE(18:0/18:2)	7,30	C41 H78 N O8 P	M-H$^-$	742.5419	742.5392	4,18	1,75	1,52	1,32	2,47
36:3	PE(18:1/18:2)	6,76	C41 H76 N O8 P	M-H$^-$	740.5246	740.5236	0,00	3,98	4,88	3,15	3,95
36:4	PE(18:2/18:2)	6,19	C41 H74 N O8 P	M-H$^-$	738.5089	738.5079	0,00	7,49	16,77	11,75	13,74
36:5	PE(18:3/18:2)	5,68	C41 H72 N O8 P	M-H$^-$	736.4934	736.4923	0,00	3,53	3,00	1,54	0,75

40:2	PE(22:0/18:2)	9,56	C45 H86 N O8 P	M-H$^-$	798.6039	798.6018	0,00	0,00	1,13	1,62	2,76
32:0	PG(16:0/16:0)	5,02	C38 H75 O10 P	M-H$^-$	721.5039	721.5025	67,34	26,93	29,36	22,41	12,06
34:1	PG(16:0/18:1)	5,48	C40 H77 O10 P	M-H$^-$	747.5189	747.5182	2,08	11,97	6,51	4,33	4,22
34:2	PG(16:0/18:2)	4,98	C40 H75 O10 P	M-H$^-$	745.5038	745.5025	26,94	27,36	37,66	43,63	45,38
34:3	PG(16:0/18:3)	4,56	C40 H73 O10 P	M-H$^-$	743.4878	743.4869	0,00	19,06	9,99	7,76	3,50
36:3	PG(18:1/18:2)	5,43	C42 H77 O10 P	M-H$^-$	771.5196	771.5182	0,56	4,49	3,19	2,97	4,14
36:4	PG(18:2/18:2)	4,92	C42 H75 O10 P	M-H$^-$	769.5034	769.5025	2,24	5,83	9,91	15,26	27,11
36:5	PG(18:2/18:3)[b]	4,37	C42 H73 O10 P	M-H$^-$	767.4884	767.4869	0,84	4,35	3,38	3,65	3,59
36:5	PG(18:3/18:2)[b]	4,54	C42 H73 O10 P	M-H$^-$	767.4874	767.4869					
34:1	PI(16:0/18:1)	4,82	C43 H81 O13 P	M-H$^-$	835.5332	835.5342	43,95	27,63	16,88	9,42	17,47
34:2	PI(16:0/18:2)	4,37	C43 H79 O13 P	M-H$^-$	833.5200	833.5186	23,51	53,42	66,46	79,02	77,43
34:3	PI(16:0/18:3)	3,97	C43 H77 O13 P	M-H$^-$	831.5052	831.5029	32,54	18,95	16,66	11,57	5,10

[a,b] regioisomeric species percentages were combined; [c] PC percentage was calculated on peak areas of $HCOO^-$ adducts

Table 3. Identification and relative abundance of GL species within each subclass in wheat kernel across T1-T5 maturation stages. Regiochemistry *sn*-1/*sn*-2 is indicated. Values (%) are means of three replicates. Relative standard deviation was lower than 10 % in all cases and is not reported. All species were detected as $HCOO^-$ adducts.

FA Group Key	Lipid Molecular Species	Base t_R (min)	Formula	Obs mass	Calc *m/z*	T1	T2	T3	T4	T5
								%		
34:1	DGDG(16:0/18:1)	6,60	C49 H90 O15	963.6278	963.6262	55,59	7,44	4,51	3,07	1,66
34:2	DGDG(16:0/18:2)	6,05	C49 H88 O15	961.6126	961.6105	0,22	21,02	23,77	24,51	28,18
34:3	DGDG(16:0/18:3)	5,57	C49 H86 O15	959.5970	959.5949	0,12	18,51	11,80	9,90	3,53
36:2	DGDG(18:1/18:1)	7,11	C51 H92 O15	989.6450	989.6418	22,06	5,27	3,73	2,58	2,97
36:3	DGDG(18:1/18:2)	6,57	C51 H90 O15	987.6281	987.6262	0,04	7,97	6,76	5,18	5,37
36:4	DGDG(18:2/18:2)	6,00	C51 H88 O15	985.6118	985.6105	21,87	13,48	23,33	28,78	47,29
36:5	DGDG(18:2/18:3)	5,49	C51 H86 O15	983.5973	983.5949	0,08	11,95	16,60	18,07	8,52
36:6	DGDG(18:3/18:3)	5,01	C51 H84 O15	981.5819	981.5792	0,00	0,49	0,40	0,31	0,18
38:3	DGDG(18:2/20:1)*	7,55	C53 H94 O15	1015.6589	1015.6575	0,01	13,87	9,11	7,59	2,30
18:2	DGMG(18:2)	1,65	C33 H58 O14	723.3825	723.3809	86,35	55,24	64,66	67,86	87,55
18:3	DGMG(18:3)	1,55	C33 H56 O14	721.3663	721.3652	13,65	44,76	35,34	32,14	12,45
34:1	MGDG(16:0/18:1)	8,04	C43 H80 O10	801.5761	801.5734	10,93	4,05	0,66	0,00	0,00
34:2	MGDG(16:0/18:2)	7,24	C43 H78 O10	799.5593	799.5577	5,30	1,95	4,76	2,77	10,79
34:3	MGDG(16:0/18:3)	6,90	C43 H76 O10	797.5436	797.5421	16,32	12,38	7,84	5,77	1,89
36:2	MGDG(18:1/18:1)	8,51	C45 H82 O10	827.5917	827.5890	55,16	3,26	2,24	1,15	1,82
36:3	MGDG(18:1/18:2)	7,93	C45 H80 O10	825.5764	825.5734	1,37	4,93	6,37	5,13	7,21

36:4	MGDG(18:2/18:2)	7,36	C45 H78 O10	823.5596	823.5577	4,44	14,56	35,72	47,01	61,86
36:5	MGDG(18:2/18:3)	6,83	C45 H76 O10	821.5444	821.5421	0,03	14,54	23,90	25,08	12,59
36:6	MGDG(18:3/18:3)	6,32	C45 H74 O10	819.5281	819.5264	6,45	44,33	18,51	13,10	3,84
18:2	MGMG(18:2)	1,89	C27 H48 O9	561.3287	561.3280	99,67	42,08	58,13	59,16	81,63
18:3	MGMG(18:3)	1,75	C27 H46 O9	559.3124	559.3124	0,33	57,92	41,87	40,84	18,37

* regiochemistry not assignable.

510 **Table 4.** Identification and relative abundance of SP species within each subclass (Cer-Ceramide; CerG1-
511 Glycosylceramide) in wheat kernel across T1-T5 maturation stages. Values (%) are means of three replicates.
512 Relative standard deviation was lower than 10 % in all cases and is not reported. All species were detected as
513 H^+ adducts.

Group Key	Lipid Molecular Species	Base t_R (min)	Formula	Obs mass	Calc *m/z*	T1	T2	T3	T4	T5
								%		
d34:0+O	Cer(t18:0/16:0)	5,91	C34 H69 N O4	556.5307	556.5299	2,17	3,10	1,18	1,68	0,33
d38:0+O	Cer(t18:0/20:0)	8,00	C38 H77 N O4	612.5930	612.5925	0,07	1,19	0,54	0,39	0,29
d40:0+O	Cer(t18:0/22:0)	9,21	C40 H81 N O4	640.6242	640.6238	6,86	6,28	2,89	2,86	2,15
d42:0+O	Cer(t18:0/24:0)	10,36	C42 H85 N O4	668.6552	668.6551	24,00	23,36	18,11	17,63	7,52
d42:0+2O	Cer(t18:0/24:0+O)	9,60	C42 H85 N O5	684.6503	684.6501	2,93	2,56	2,18	3,53	5,83
d42:1+O	Cer(t18:0/24:1)	9,51	C42 H83 N O4	666.6397	666.6395	19,80	18,77	15,27	12,64	17,10
d43:0+O	Cer(t18:0/25:0)	11,06	C43 H87 N O4	682.6713	682.6708	1,46	1,30	0,23	0,35	0,31
d44:0+O	Cer(t18:0/26:0)	11,67	C44 H89 N O4	696.6870	696.6864	5,83	3,60	3,76	4,02	10,15
d34:0	Cer(d18:0/16:0)	6,85	C34 H69 N O3	540.5359	540.5350	0,06	1,02	2,51	2,27	1,17
d34:0+O	Cer(d18:0/16:0+O)	6,18	C34 H69 N O4	556.5307	556.5299	0,00	0,95	2,30	0,54	0,02
d36:2	Cer(d18:0/18:2)	6,88	C36 H69 N O3	564.5358	564.5350	0,10	0,40	2,17	3,54	1,12
d42:1+O	Cer(t18:1/24:0)	9,59	C42 H83 N O4	666.6393	666.6395	6,92	5,46	5,18	5,50	8,84
d42:1+2O	Cer(t18:1/24:0+O)	9,53	C42 H83 N O5	682.6351	682.6344	5,71	5,72	3,10	4,61	3,67
d34:1+O	Cer(d18:1/16:0+O)	4,76	C34 H67 N O4	554.5152	554.5143	0,02	1,68	13,14	14,49	10,59
d36:3	Cer(d18:1/18:2)	6,55	C36 H67 N O3	562.5203	562.5194	0,00	0,61	2,30	3,80	0,35
d38:1+O	Cer(d18:1/20:0+O)	8,01	C38 H75 N O4	610.5775	610.5769	1,87	1,27	3,41	2,47	2,57
d42:1+O	Cer(d18:1/24:0+O)	9,65	C42 H83 N O4	666.6393	666.6395	17,47	17,98	14,07	11,57	14,94
d34:3	Cer(d18:2/16:1)	4,54	C34 H63 N O3	534.4891	534.4881	0,48	1,41	3,49	3,16	1,78
d42:2+O	Cer(d18:2/24:0+O)	9,44	C42 H81 N O4	664.6244	664.6238	1,85	2,11	1,05	1,01	1,25
d38:1+O	Cer(d20:1/18:0+O)	6,73	C38 H75 N O4	610.5774	610.5769	2,40	1,23	3,11	3,93	10,00

d40:1+2O	CerG1(t18:1/22:0+O)	7,20	C46 H89 N O10	816.6570	816.6559	0,69	6,86	1,20	0,00	0,89
d42:1+2O	CerG1(t18:1/24:0+O)	8,31	C48 H93 N O10	844.6880	844.6872	45,21	19,89	3,95	3,52	0,20
d34:1+O	CerG1(d18:1/16:0+O)	4,76	C40 H77 N O9	716.5681	716.5671	20,71	18,79	42,65	43,80	32,80
d34:2	CerG1(d18:1/16:1)	4,80	C40 H75 N O8	698.5573	698.5565	1,18	4,96	1,71	1,33	0,67
d38:1+O	CerG1(d18:1/20:0+O)	6,73	C44 H85 N O9	772.6303	772.6297	2,23	2,25	6,50	8,71	22,15
d34:2+O	CerG1(d18:2/16:0+O)	4,54	C40 H75 N O9	714.5523	714.5515	20,81	19,24	16,01	14,32	7,66
d34:3	CerG1(d18:2/16:1)	4,54	C40 H73 N O8	696.5417	696.5409	0,03	15,99	13,24	11,64	6,48
d38:2+O	CerG1(d18:2/20:0+O)	6,52	C44 H83 N O9	770.6145	770.6141	7,78	5,94	5,39	5,69	4,22
d38:3	CerG1(d18:2/20:1)	6,51	C44 H81 N O8	752.6047	752.6035	0,00	3,62	3,05	3,29	2,77
d38:1+O	CerG1(t20:0/18:1)	6,72	C44 H85 N O9	772.6303	772.6297	1,36	2,45	6,30	7,71	22,15

514

515

Figure captions

Fig. 1. Representative structures of main lipids other than simple acylglycerols identified in durum wheat kernel.

Fig. 2. UHPLC-ESI-MS/MS-based TAG species profile of wheat kernels across T1-T5 maturation stages. Peak areas were compared on kernel dry weight basis. Values are average of three replicates. Standard deviation was always below 10 % and was not reported.

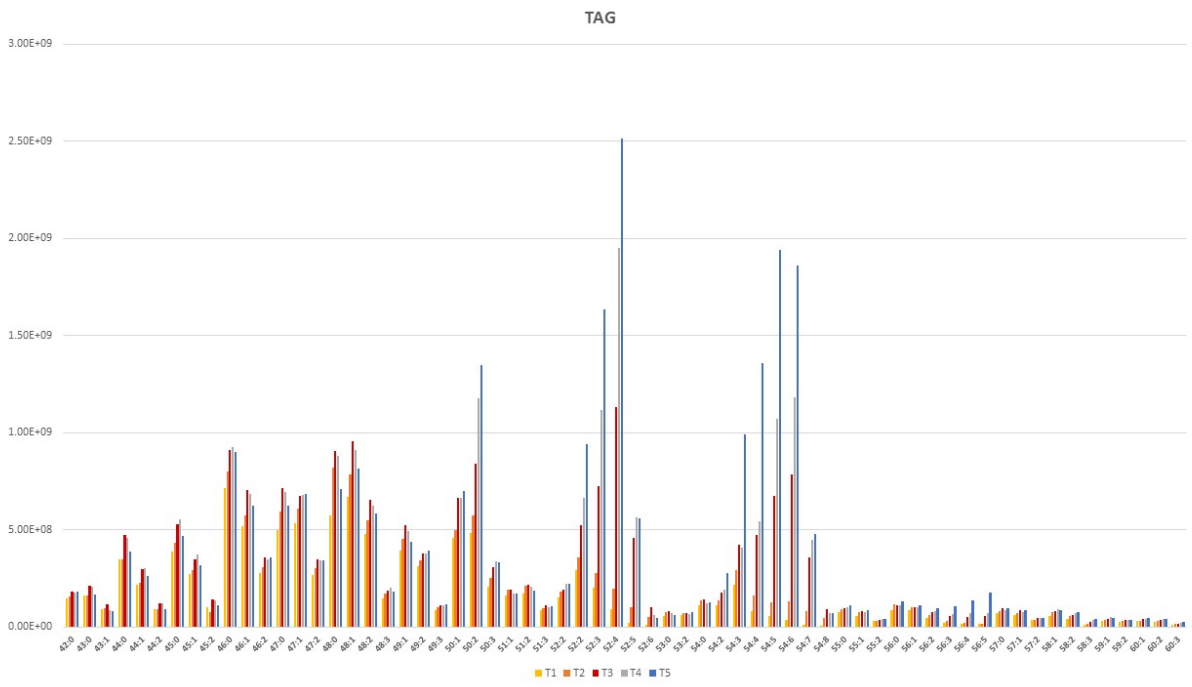
TAG
3.00E+09
2.50E+09
2.00E+09
1.50E+09
1.00E+09
5.00E+08
0.00E+00
T1
T2
T3
T4
T5

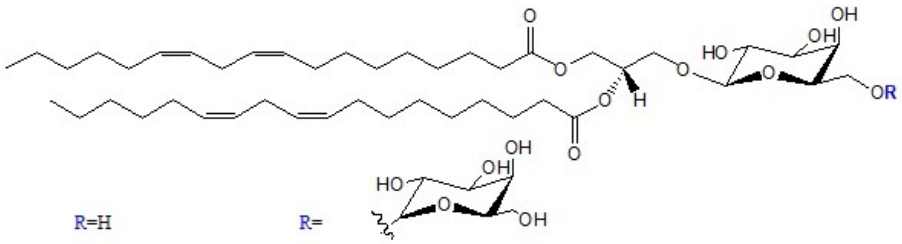

R=H

R=

MGDG (18:2/18:2) **DGDG (18:2/18:2)**

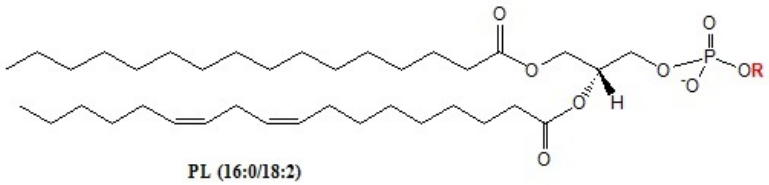

PL (16:0/18:2)

R=

-H **PA**

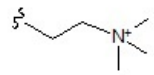

PC

PE

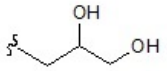

PG

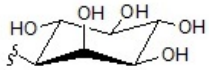

PI

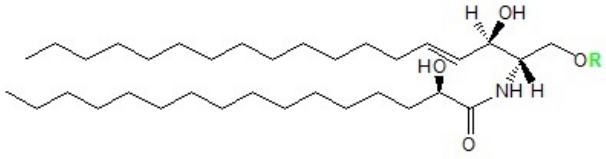

R=H

R=

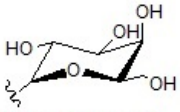

Cer d18:1/16:0(2OH) **GlcCer d18:1/16:0(2OH)**

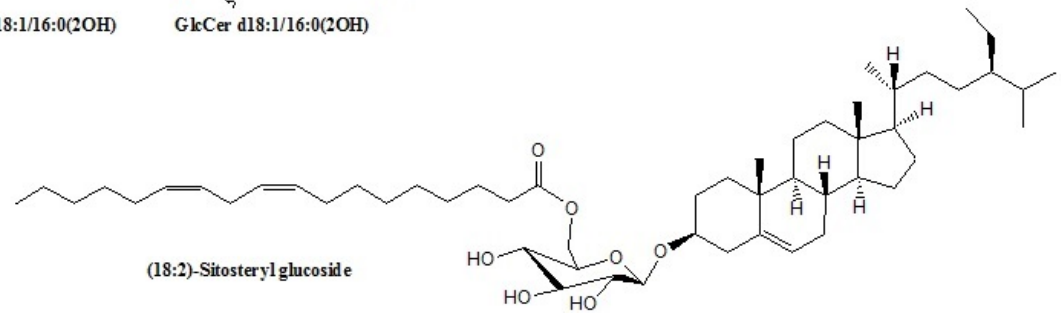

(18:2)-Sitosteryl glucoside

- Grain kernels were harvested at 5 key stages of development (5-30 days post anthesis)

- Lipidome evolution was assessed during kernel filling by UHPLC-Q Exactive-MS/MS

- Triacylglycerols and polar lipids steadily accumulated, while fatty acids declined

- Linoleic acid dominated in all glycerolipids

- Lipidomics of growing kernels complements the biomolecular inventory of durum wheat

Declaration of interests

☒ The authors declare that they have no known competing financial interests or personal relationships that could have appeared to influence the work reported in this paper.

☐The authors declare the following financial interests/personal relationships which may be considered as potential competing interests: